JACS
JOURNAL OF THE AMERICAN CHEMICAL SOCIETY

Communication

pubs.acs.org/JACS

$Cu_2ZnSnS_{4x}Se_{4(1-x)}$ Solar Cells from Polar Nanocrystal Inks

Joel van Embden,* Anthony S. R. Chesman, Enrico Della Gaspera, Noel W. Duffy, Scott E. Watkins, and Jacek J. Jasieniak*

CSIRO Materials Science and Engineering, Bayview Avenue, Clayton, Victoria 3168, Australia

Supporting Information

ABSTRACT: A facile ligand exchange method for dispersing Cu_2ZnSnS_4 (CZTS) nanocrystals (NCs) in environmentally benign polar solvents, such as ethanol or *n*-propanol, at high concentrations (up to 200 mg/mL) is demonstrated. This approach has been applied to CZTS nanocrystals synthesized via scalable, noninjection methods to formulate colloidally stable inks that are suitable for the solution processing of solar cell devices. Unlike other inks currently used to fabricate NC solar cells, the CZTS nanocrystal ink developed here circumvents the need for hydrazine, pyridine, or thiol coordinating solvents. By combining our polar CZTS inks with optimized selenization procedures, substrate CZTSSe solar cells have been successfully fabricated with device efficiencies of 7.7%.

The eventual uptake of solution processed solar cells by the renewable energy market hinges upon both the ability to synthesize the required semiconductor "ink" dispersions using scalable low cost methods as well as the processing of these inks into devices using simple, benign chemistry. Recently, $Cu_2ZnSnS_{4x}Se_{4(1-x)}$ (CZTSSe) has emerged as one of the most promising candidates for use as the absorber layer in such devices because of its ideal bad gap, low cost, and the high earth abundance of its elemental components.[1] To date, among the highest efficiency CZTSSe solar cells are those made from molecular precursor solutions[2−4] or NC dispersions.[5−8] Although molecular-based inks are appealing because of their ready scalability, they are compromised by the necessity of having to use highly toxic solvents, such as hydrazine,[8,9] or metal−organic precursors that contain extremely high concentrations of organic contaminants in order to generate stable dispersions.[4,10]

Nanocrystal-based inks offer an excellent alternative to these approaches. In this regard numerous semiconductor NCs have emerged as either proven[3,11−13] or potential[1,14−16] absorber layer materials. Provided that such NCs are made using noninjection techniques, they become directly competitive with molecular-based inks for commercial scale application. Furthermore, the labile surface chemistry of NCs permits the native ligands used during synthesis to be readily exchanged with shorter chain ligands of the desired functionality.[17,18] This enables the ability to reduce the organic component and also permits their dispersion in a variety of desirable solvents. Surprisingly, these advantages have been underexploited for ternary and quaternary NC systems.

Here we show for the first time the fabrication of highly efficient CZTSSe NC-based solar cells processed from a benign polar solvent system (1-propanol). The simple method developed here avoids the use of toxic and pungent pyridine[11,19] and thiol based solvents,[5,6,13,20] which to date have been required to afford NC solar cells with high efficiencies. Polar (CZTS) NC inks have the added advantage that they permit the direct solubilization of beneficial dopants, such as sodium,[13,21] potassium,[22] and antimony[23] in controllable amounts. Such NC inks have the potential to circumvent the need for post deposition dopant incorporation[13,23,24] or complicated syntheses that aim to dope the surface of CZTS NCs.[7] In general, the results presented herein open a window to the development of more complex NC ink formulations.

Scheme 1. Fabrication of a CZTSSe Solar Cell Utilizing a Scalable Polar NC Ink

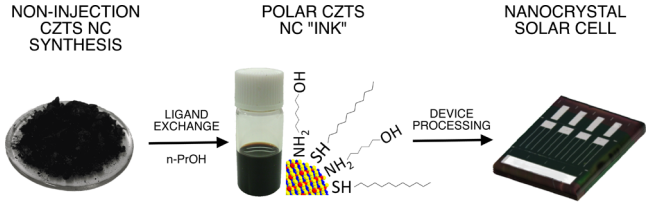

CZTS nanocrystals were synthesized according to a noninjection method developed by our group.[25] The reaction pathway used employs two distinct in situ generated metal sulfide precursors, which enable complete temporal separation of the nucleation and growth stages of the reaction. In this way CZTS NCs with a tight size distribution and compositional control can be made on multigram scales.[25,26] For our study we chose to use copper deficient NCs with elemental ratios of Cu/(Zn + Sn) = 0.85 and Zn/Sn = 1.12, on the basis of previously reported optimal compositions.[3] The as-prepared CZTS NCs were purified and ligand exchanged with 5-amino-1-pentanol (AP). For details on the ligand exchange and solvent transfer, see the Supporting Information. The dry exchanged NCs were then combined with anhydrous *n*-PrOH to afford the final CZTS ink (~140 mg/mL). This ink was found to be stable for months without aggregation.

Thin films of CZTS NCs were deposited using a layer-by-layer (LbL) approach.[11] Several layers were spin coated on molybdenum coated glass substrates. After each deposition the films were annealed for 5 min at 350 °C under an N_2

Received: February 4, 2014
Published: April 1, 2014

dx.doi.org/10.1021/ja501218u | J. Am. Chem. Soc. 2014, 136, 5237−5240

atmosphere. This temperature was selected on the basis of Fourier transform infrared (FTIR) spectroscopy of thin films heated at various temperatures (Figure 1A). These measurements showed that heat treatment at 350 °C was sufficient to remove >95% of the aliphatic impurities. Although higher temperatures could be utilized to achieve even purer films, this temperature was selected for our studies to avoid extraneous sulfur loss.

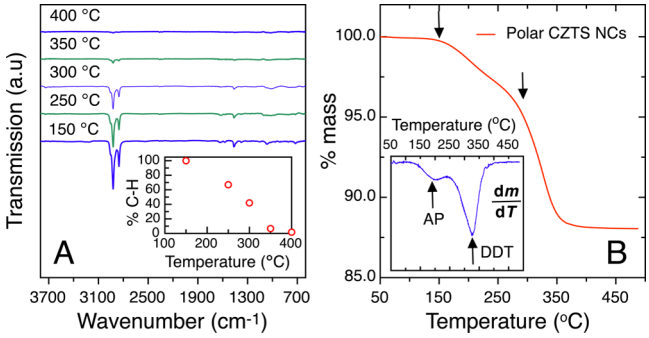

Figure 1. (A) FTIR of CZTS NC films annealed at various temperatures for 5 min under N_2. Integrated analysis (inset) confirms a relative 96% reduction in the organic signal after annealing the NC films at 350 °C. (B) TGA of the dried polar ink performed under N_2 showing a total 12% mass loss by 350 °C, after which negligible mass loss is evident. The inset shows the derivative spectrum highlighting the mass loss results from two distinct species (see arrows), specifically 5-amino-1-pentanol (AP) and 1-dodecanethiol (DDT). See Supporting Information for detailed analysis.

To compliment these results, thermogravimetric analysis (TGA) of the CZTS NCs used in this work was performed (Figure 1B). A total 12% mass loss was observed between 50 and 350 °C, with no further reduction in mass occurring as the temperature was raised to 500 °C. This confirms near complete volatilization of surface ligands by ~350 °C. Importantly, the TGA shows two distinct mass loss regions at ~150 and 270 °C (see arrows), which corresponds to AP and dodecanethiol (DDT) volatilization, respectively (see also Figure S1, Supporting Information). From the integrated analysis of the d*m*/d*T* plot (see Figure 1B inset) we estimate that the surface coverage of the CZTS NCs consists of 56% AP and 44% DDT by number. This highlights that amines and thiols bind strongly to distinct subsets of atoms on the CZTS surface. As further confirmation of this, the AP was found to completely displace the original oleylamine ligands on the surface (see Figure S1). Remarkably, this mixed surface ligand shell provides a sufficiently high polarity to reliably disperse the nanocrystals in various polar solvents at concentrations up to 200 mg/mL.

Ultimately, optimization of the p-type CZTS NC layer is the most critical parameter to realize high efficiency solar cell devices. CZTS NC thin films prepared via the aforementioned heat treatment procedure have low surface ligand coverage, but still maintain poor optoelectronic properties.[27,28] This arises from the large number of grain boundaries present with the NC films. To induce grain growth and reduce the residual impurities, the CZTS NC films were rapidly heated to high temperatures in the presence of a high vapor pressure of selenium. Unlike cation exchange, which occurs via diffusion through interstitial sites within the lattice, the formation of a sulfoselenide compound induces large-scale grain growth due to the dissolution and reformation of the anion-based lattice. The grain growth associated with the selenization process is known to enhance the photoconductivity of CZTS NC films, indicating improved optoelectronic properties.[27] The selenization process outlined here was conducted by loading the preannealed films into a cylindrical graphite box (6 cm^3 internal free volume per film, 100 mg of Se pellets per film), which was then placed in a tube furnace. After several pump/purge cycles to remove the air, the furnace was rapidly heated (~50 °C/min) to the desired temperature under ~1 atm of argon in order to generate a high vapor pressure of selenium.

Figure 2A shows cross-sectional scanning electron microscope (SEM) images of the representative changes that occur in the morphology of the CZTS NC layer over time under our optimized selenization conditions. The CZTS NC films with initial thicknesses of 520 nm were heated over 10 min to 450 °C and then maintained at this temperature for different time periods. It was found that longer selenization times resulted in a thicker "large grain" top layer and a reduction in the "fine grain" nanocrystalline underlayer. After 40 min at 450 °C single 550–600 nm CZTSSe grains are observed, as well as a thin (130 nm) nanocrystalline underlayer. Heating for longer periods resulted in no further reduction to this underlayer (see Figure S2), which is known to be carbon and selenium rich.[29] It should be noted that similar trends were observed at higher temperatures (up to 500 °C), although shorter times were required to achieve comparable grain growth. Interestingly, regardless of the initial NC film thickness, the large grain layer could not be grown beyond 600–650 nm. Thicker initial NC films simply resulted in a thicker underlayer. This phenomenon is common to the selenization of all CZTS and CIGS NC thin films to date[5,6,13,29,30] and presents perhaps the most significant challenge to future progress in the field of NC-based optoelectronics.

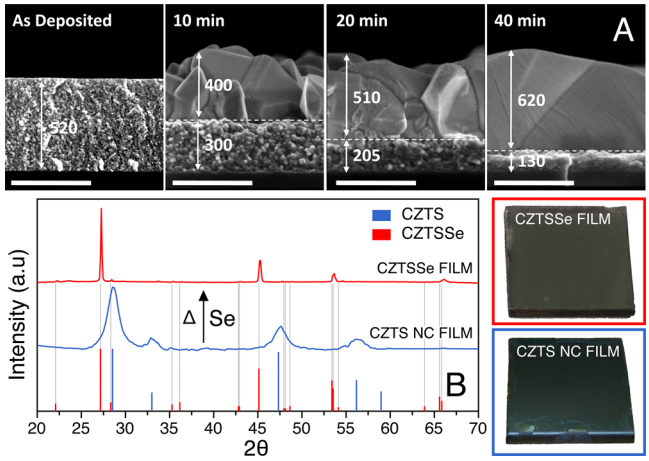

Figure 2. (A) SEM images of a CZTS NC film after various selenization times at 450 °C. Large grains and minimization of the fine grain underlayer is achieved after 40 min. Scale bars are 500 nm. (B) XRD patterns of an as-deposited CZTS NC film and a typical selenized CZTSSe film (40 min @ 450 °C) on silicon substrates (data plotted on a square root scale). The dotted lines aid in the assignment of smaller peaks observed for the selenized film. Photos of typical CZTS NC film before (blue) and after selenization (red) are shown for reference. While the as-deposited CZTS NC film appears smooth and black in color, the selenized sample displays a homogeneous gray/green color and is highly scattering.

dx.doi.org/10.1021/ja501218u | J. Am. Chem. Soc. 2014, 136, 5237–5240

To confirm the phase purity of the selenized films, X-ray diffraction (XRD) was performed. Figure 2B shows that the selenization process induces both shifting and sharpening of the diffraction peaks, which are associated with the expansion of the lattice following selenium incorporation and a $\sim 10^2$ fold increase in domain size, respectively. All the peaks in the pure CZTS NC film and the selenized sample can be assigned to bulk kesterite CZTS (ICDD No. 00-026-0575) and CZTSe (ICDD No. 04-010-6295) respectively, although in the case of the selenized sample a slight shift of the reflections to higher angles is observed because of the presence of residual sulfur in the lattice. Vegard analysis of the peak positions in the CZTSSe film confirms ~90% anion exchange between sulfur and selenium occurs during selenization.

XRD alone is incapable of adequately identifying the presence of secondary phases, such as ZnS, which are known to phase separate at high temperatures under nonideal conditions.[31] As such, Raman spectroscopy was also performed on the selenized films (see Figure S3). Importantly, both XRD and Raman analyses confirmed that no major crystalline secondary phases were generated under our optimized selenization conditions.

The resulting kesterite CZTSSe layers were fabricated into solar cell devices by depositing a 50 nm thick n-type CdS layer using a chemical bath, followed by the sputtering of a 40 nm thick *i*-ZnO and a 150 nm thick ITO (~30 Ω/□) transparent conductive electrode (TCE) stack. Thermal evaporation of aluminum through a shadow mask was then performed, which served as a charge collection grid. The final devices were defined by mechanical scribing to provide total (active) areas of 0.5 cm^2 (0.37 cm^2). For details of these procedures, see the Supporting Information (Figure S4). Notably, prior to CdS deposition, the selenized films were etched in a 0.4 M aqueous HCl solution for 5 min. This treatment was found to etch residual surface contaminants from the selenization procedure.[32] This process was necessary to realize a clean interface at the p−n junction, which was found to improve both device performance and reproducibility.

Figure 3A,B shows cross-sectional SEM images of the final device (Mo/CZTSSe/CdS/*i*-ZnO/ITO/Al) and the p−n junction/TCE interfaces, respectively. For a more detailed view of the substrate, see Figure S5. The different layers present within the device have been color coded for clarity. The Mo/$MoSe_2$ substrate (blue) is composed of Mo (300 nm) and $MoSe_2$ (190 nm). The p-type CZTSSe layer (850−900 nm) may be divided into a "large grain" top layer (~550 nm, brown) as well as a "fine grain" underlayer (~350 nm, red). The CdS window layer (~50 nm, green), *i*-ZnO (~40 nm, purple), and ITO (150 nm, white) are also highlighted. While the interface between the CZTSSe layer and the sintered underlayer may be considered structurally nonideal, each of the interfaces surrounding the p−n junction are seen to be of a high quality (Figure 3B).

Figure 3C shows the light and dark current−voltage curves of the champion cell under AM 1.5G illumination. V_{OC} = 0.41 V, J_{SC} = 32.9 mA/cm^2, FF = 56.9%, and an active area PCE of 7.68% are calculated. Analysis of the *J*−*V* curves through a modified Shockley-diode equation (see Figure S7), yielded a high dark shunt resistance (R_{SH}) of 710 Ω cm^2, a series resistance (R_S) of 1.45 Ω cm^2, a saturation current (J_0) of 2.1 × 10^{-5} A/cm^2, and a diode quality factor (n) of 1.82. Notably, from 12 measured devices, 11 exhibited similar device parameters and PCE values greater than 6.0%, highlighting

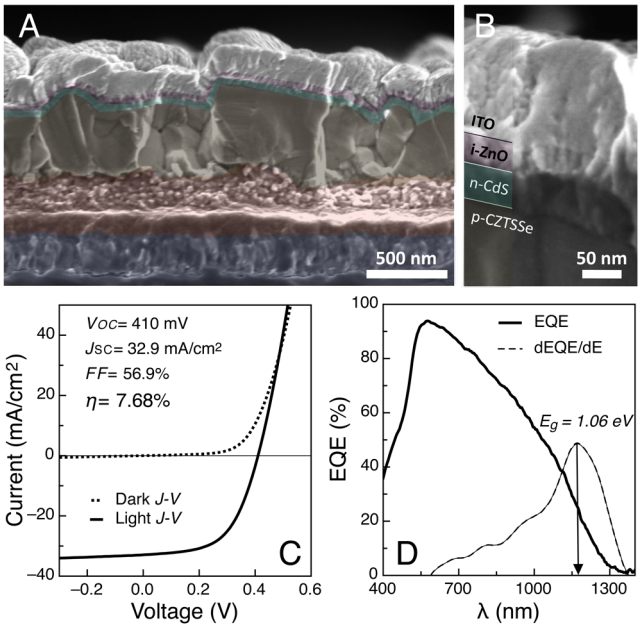

Cell Param.	R_S (Ω·cm2)	R_{SH} (Ω·cm2)	J_0 (A/cm2)	n
Value	1.45	710	2.1×10-5	1.82

Figure 3. (A) Cross-sectional SEM of the champion device. For a view of the uncolored SEM image, see Figure S6. (B) High-resolution SEM image highlighting the p−n junction and TCE layers. (C) Light and dark current/voltage curves for the champion cell. (D) The EQE of a sister cell to the champion cell. The band gap has been estimated as 1.06 eV. Fitted cell statistics are shown in the table (see also Figure S7).

the robust nature of the processing conditions employed here. The overall device performance observed for these solar cells is very encouraging, even at this early stage in the exploitation of the possibilities associated with polar NC inks. Notably, the devices fabricated here have been made without an antireflective coating. The device characteristics are directly comparable to CZTS NC-based solar cells that are currently prepared using toxic and pungent thiol based solvents,[5,6,13,20] with the considerable advantage of being processed from a benign solvent/ligand combination that is conducive to printing.

Examination of the EQE data reveals a peak photocurrent efficiency of >90% at ~600 nm, below which strong losses resulting from CdS absorption are observed. A gradual decay in photocurrent is also seen at longer wavelengths. This factor is likely a consequence of (i) a less than optimal CZTSSe thickness, which leads to reduced absorption in this region, and (ii) higher recombination losses for low energy photons that are absorbed close to or within the "fine grain" underlayer. Deeper insight into the resistive effect of this fine grain layer can be gleaned by examination of a device with duplicate selenized layers (see Figure S8 for details). From the peak in the dEQE/dE plot, we estimate the absorber band gap in the solar cells at 1.06 eV. This is consistent with the observed XRD data for a nearly pure CZTSe p-type absorber layer.[33] When compared to the V_{oc}, a total voltage deficit of ~650 meV is determined, similar to current record CZTSSe devices.[3] The relatively high value of the voltage deficit is indicative of midgap trap states (recombination centers) present within the devices,[34] which is supported by the moderately high J_0 and n parameters. It is anticipated that each of the above

dx.doi.org/10.1021/ja501218u | J. Am. Chem. Soc. 2014, 136, 5237−5240

observations can be addressed by optimization of the CZTSSe mircostructure, to achieve a thicker "large grain" component of the absorbing layer, and through grain boundary engineering.[35]

In conclusion, we have demonstrated a facile ligand exchange process for CZTS NCs that enables their dispersion in environmentally friendly polar solvents. Additional significance is placed on the fact that these dispersions were formulated using NCs synthesized via a scalable, noninjection-based technique. The results presented highlight the viability of using polar NC ink dispersions to achieve high performing (>7%) CZTSSe solar cells without the need for toxic or pungent solvents. Further improvements to device performance will require developing methods to manipulate the CZTSSe microstructure and grain-boundaries. Tackling this challenge will be greatly facilitated by the use of polar NC inks, whose composition may be tailored through the codissolution of beneficial dopants and growth promoting additives.

■ ASSOCIATED CONTENT

Supporting Information

Further experimental details, spectra, and microscopy. This material is available free of charge via the Internet at http://pubs.acs.org.

■ AUTHOR INFORMATION

Corresponding Author

joel.vanembden@csiro.au; jacek.jasieniak@csiro.au

Notes

The authors declare no competing financial interest.

■ ACKNOWLEDGMENTS

This work was funded through the Flexible Electronics Theme of the Future Manufacturing Flagship as part of an Office of the Chief Executive Postdoctoral Fellowship. The authors acknowledge the Australian Research Council for support through the Grant DP110105341 and a DECRA. This work was partially supported by funding from the Australian Renewable Energy Agency through the Australian Centre for Advanced Photovoltaics.

■ REFERENCES

(1) Wadia, C.; Alivisatos, A.; Kammen, D. *Environ. Sci. Technol.* **2009**, *43*, 2072.

(2) Schnabel, T.; Löw, M.; Ahlswede, E. *Sol. Energy Mater. Sol. Cells* **2013**, *117*, 324.

(3) Wang, W.; Winkler, M. T.; Gunawan, O.; Gokmen, T.; Todorov, T. K.; Zhu, Y.; Mitzi, D. B. *Adv. Energy Mater.* **2013**, DOI: 10.1002/aenm.201301465.

(4) Wang, G.; Zhao, W.; Cui, Y.; Tian, Q.; Gao, S.; Huang, L.; Pan, D. *ACS Appl. Mater. Interfaces* **2013**, *5*, 10042.

(5) Guo, Q.; Ford, G.; Yang, W.-C.; Walker, B.; Stach, E.; Hillhouse, H.; Agrawal, R. *J. Am. Chem. Soc.* **2010**, *132*, 17384.

(6) Cao, Y.; Denny, M. S.; Caspar, J. V.; Farneth, W. E.; Guo, Q.; Ionkin, A. S.; Johnson, L. K.; Lu, M.; Malajovich, I.; Radu, D.; Rosenfeld, H. D.; Choudhury, K. R.; Wu, W. *J. Am. Chem. Soc.* **2012**, *134*, 15644.

(7) Zhou, H.; Song, T.-B.; Hsu, W.-C.; Luo, S.; Ye, S.; Duan, H.-S.; Hsu, C.-J.; Yang, W.; Yang, Y. *J. Am. Chem. Soc.* **2013**, *135*, 15998.

(8) Yang, W.; Duan, H.-S.; Bob, B.; Zhou, H.; Lei, B.; Chung, C.-H.; Li, S.-H.; Hou, W.; Yang, Y. *Adv. Mater.* **2012**, *24*, 6323.

(9) Todorov, T.; Reuter, K.; Mitzi, D. *Adv. Mater.* **2010**, *22*, E156.

(10) Cho, J.; Ismail, A.; Park, S.; Kim, W.; Yoon, S.; Min, B. *ACS Appl. Mater. Interfaces* **2013**, *5*, 4162.

(11) Jasieniak, J.; MacDonald, B. I.; Watkins, S. E.; Mulvaney, P. *Nano Lett.* **2011**, *11*, 2856.

(12) Hillhouse, H. W.; Beard, M. C. *Curr. Opin. Colloid Interface Sci.* **2009**, *14*, 245.

(13) Guo, Q.; Ford, G. M.; Agrawal, R.; Hillhouse, H. W. *Prog. Photovoltaics* **2013**, *21*, 64.

(14) van Embden, J.; Latham, K.; Duffy, N. W.; Tachibana, Y. *J. Am. Chem. Soc.* **2013**, *135*, 11562.

(15) Norako, M. E.; Greaney, M. J.; Brutchey, R. L. *J. Am. Chem. Soc.* **2012**, *134*, 23.

(16) van Embden, J.; Yasuhiro, T. *J. Mater. Chem.* **2012**, *22*, 11466.

(17) Bullen, C.; Mulvaney, P. *Langmuir* **2006**, *22*, 3007.

(18) Petruska, M. A.; Malko, A. V.; Voyles, P. M.; Klimov, V. I. *Adv. Mater.* **2003**, *15*, 610.

(19) Panthani, M.; Kurley, J.; Crisp, R.; Dietz, T.; Ezzyat, T.; Luther, J.; Talapin, D. *Nano Lett.* **2014**, DOI: 10.1021/nl403912w.

(20) Ford, G. M.; Guo, Q.; Agrawal, R.; Hillhouse, H. W. *Chem. Mater.* **2011**, *23*, 2626.

(21) Prabhakar, T.; Jampana, N. *Sol. Energy Mater. Sol. Cells* **2011**, *95*, 1001.

(22) Chirila, A.; Reinhard, P.; Pianezzi, F.; Bloesch, P.; Uhl, A.; Fella, C.; Kranz, L.; Keller, D.; Gretener, C.; Hagendorfer, H.; Jaeger, D.; Erni, R.; Nishiwaki, S.; Buecheler, S.; Tiwari, A. *Nat. Mater.* **2013**, *12*, 1107.

(23) Carrete, A.; Shavel, A.; Fontan, X.; Montserrat, J.; Fan, J.; Ibanez, M.; Saucedo, E.; Perez-Rodreguez, A.; Cabot, A. *J. Am. Chem. Soc.* **2013**, *135*, 15982.

(24) Rudmann, D.; da Cunha, A. F.; Kaelin, M.; Kurdesau, F.; Zogg, H.; Tiwari, A. N.; Bilger, G. *Appl. Phys. Lett.* **2004**, *84*, 1129.

(25) Chesman, A. S. R.; van Embden, J.; Duffy, N. W.; Webster, N. A. S.; Jasieniak, J. J. *Cryst. Growth Des.* **2013**, *13*, 1712.

(26) Chesman, A. S. R.; Duffy, N. W.; Peacock, S.; Waddington, L.; Webster, N. A. S.; Jasieniak, J. J. *RSC Adv.* **2013**, *3*, 1017.

(27) Riha, S.; Fredrick, S.; Sambur, J.; Liu, Y.; Prieto, A.; Parkinson, B. *ACS Appl. Mater. Interfaces* **2011**, *3*, 58.

(28) Steinhagen, C.; Panthani, M.; Akhavan, V.; Goodfellow, B.; Koo, B.; Korgel, B. *J. Am. Chem. Soc.* **2009**, *131*, 12554.

(29) Hages, C. J.; Levcenco, S.; Miskin, C. K.; Alsmeier, J. H.; Abou-Ras, D.; Wilks, R. G.; Bar, M.; Unold, T.; Rakesh, A. *Prog. Photovoltaics* **2013**, DOI: 10.1002/pip.2442.

(30) Ahn, S.; Choi, Y.; Kim, K.; Eo, Y.-J.; Cho, A.; Gwak, J.; Yun, J.; Shin, K.; Ahn, S.; Yoon, K. *ChemSusChem* **2013**, *6*, 1282.

(31) Scragg, J. J.; Watjen, J. T.; Edoff, M.; Ericson, T.; Kubart, T.; Platzer-Bjorkman, C. *J. Am. Chem. Soc.* **2012**, *134*, 19330.

(32) Fairbrother, A.; Garcia-Hemme, E.; Izquierdo-Roca, V.; Fontane, X.; Pulgarin-Agudelo, F. A.; Vigil-Galan, O.; Perez-Rodriguez, A.; Saucedo, E. *J. Am. Chem. Soc.* **2012**, *134*, 8018.

(33) Bag, S.; Gunawan, O.; Gokmen, T.; Zhu, Y.; Todorov, T. K.; Mitzi, D. B. *Energy Environ. Sci.* **2012**, *5*, 7060.

(34) Mitzi, D. B.; Gunawan, O.; Todorov, T. K.; Barkhouse, D. A. R. *Philos. Trans. R. Soc., A* **2013**, *100*, 20110432.

(35) Yin, W.-J.; Wu, Y.; Wei, S.-H.; Noufi, R.; Al-Jassim, M. M.; Yan, Y. *Adv. Energy Mater.* **2014**, *4*, 1300712.